

Imaging Colorimetry Using a Digital Camera*

Wencheng Wu and Jan P. Allebach
School of ECE, Purdue University, West Lafayette, Indiana
Mostafa Analoui
School of Dentistry, Indiana University, Indianapolis, Indiana

Abstract

In this paper, we investigate a multi-exposure multi-illuminant colorimetry system using a Kodak DCS460c digital camera. Our system consists of a measurement device and calibration matrices. The measurement device is formed by a digital camera and a set of filters, and the term multi-exposure refers to the multiple snapshots taken by this camera using different filters. The calibration matrices then take these filtered camera RGB outputs, and return the CIE XYZ tristimulus values under several pre-selected illumination conditions. Our objective is to find the optimal filters and the corresponding calibration matrices that minimize a cost function accounting for errors in $L^*a^*b^*$ space, system robustness, and filter smoothness.

We applied this methodology and implemented a two-exposure camera system using Wratten filters. The experimental results are presented in this paper.

1. Introduction

Accurate assessment of color is essential in many applications. A colorimetry system is designed to serve this purpose by providing tristimulus values for a given color stimulus. Colorimetry systems often consist of a measurement device, and a corresponding calibration mapping. Based on the intrinsic differences in the mechanism of the measurement device, there are three types of colorimetry systems, the spectroradiometer, the spectrophotometer, and the tristimulus-filter colorimeter.[1] Both the spectroradiometer and spectrophotometer provide spectral measurements of the sample over the range of visible wavelengths. Then the tristimulus values can be obtained by using the color matching functions of the CIE standard colorimetric observer.[1] The tristimulus-filter colorimeter on the other hand provides only the tristimulus values of a sample; and its calibration mapping is nontrivial when the measurement device is not colorimetric.

However, there are several advantages of the tristimulus-filter type colorimeter over radiometric type systems when it is properly designed. First of all, radiometric systems typically yield only spot measurements. A tristimulus-filter type colorimeter can have high spatial resolution, especially if a mega-pixel digital camera is used as the measurement device. Secondly, colorimeters are easier to set up and operate. Finally, the measurement device in the tristimulus-filter colorimeter is flexible and can be readily implemented using popular low cost imaging devices such as scanners[2] or digital cameras.[3]

In this paper, we propose the multi-exposure camera system shown in Fig. 1 for imaging colorimetry. Since the calibration matrix $\boldsymbol{M}'$ is an illuminant-dependent module whose illumination condition $\boldsymbol{L}'$ need not be the same as the illuminant $\boldsymbol{L}$ under which the measurements are made, it is straightforward to extend this system to multiple illuminants.

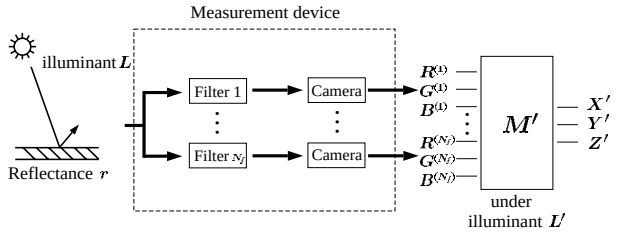

$\boldsymbol{r}$: 31-*pt. reflectance*
$\boldsymbol{L}$: 31×31 *diagonal illuminant matrix*
$\boldsymbol{f}_i$: 31-*pt. filter transmittance of* i*th filter*
$\boldsymbol{D}$: 31×3 *camera sensitivity matrix*
N_f : *number of exposures in measurement device*
$\boldsymbol{M}'$: $3N_f \times 3$ *calibration matrix under illuminant* $\boldsymbol{L}'$
$\boldsymbol{A}$: 31×3 *CIE XYZ color matching functions*

Figure 1: *Multi-exposure single-illuminant colorimetry system*

Similar to most colorimetric devices, our system contains both the measurement device and the calibration mapping. The measurement device is a multi-exposure camera system composed of filters and a digital camera. The filters are used to increase the number of measurement channels, thereby improving the precision of the color calibration.[3] We then design a set of illuminant-dependent calibration matrices to estimate the CIE XYZ tristimulus values under several different illuminants. Instead of reconstructing

*Research supported by a grant from Purdue Research Foundation and the School of Dentistry at Indiana University

the reflectance of a color sample,[3,4] our goal is to obtain the tristimulus values of a color sample under several pre-selected illumination conditions. In essence when the set of pre-selected illuminants is large enough, this method is equivalent to methods that reconstruct the reflectance of a sample. However, unlike reflectance reconstruction methods which weight equally all possible lighting conditions, the strategy of this method is to focus on reducing the colorimetric errors more under those lighting conditions that are frequently encountered and less under those that are not. As a result, a more efficient calibration system can be developed.

Much work has been done on designing the calibration mapping for given devices. One common technique uses a matrix transformation to map device outputs into a desired space. Our previous work[5] applied a regression method to a set of camera measurements to find the optimal calibration matrix which minimized the errors in CIE XYZ space. Farrell et al[2] employed the same method to turn scanners into colorimeters. Alternatively, one can employ a model of the device to design a suitable calibration matrix. Finlayson and Drew[6] utilized the spectral sensitivities of the measurement device and an assumption regarding sample reflectances to find the calibration matrix.

For the measurement device, Chen and Trussell[7] used filters to alter the device sensitivities and designed an optimal filter set that maximizes Vora's measure of goodness. Tominaga[3] and Haneishi et al[4] used filters along with a monochrome CCD camera to increase the number of device channels. Wolski et al[8] designed a colorimeter by a combination of LEDs, filters, and a common detector. In Ref. 3, the filters are selected from a set of narrow-band Wratten filters. In both Refs. 4 and 7, the filters are restricted to a Gaussian shape. The design problems are all formulated in such a way that the optimal filter set maximizes the system performance under a given metric. However, only Ref. 8 takes system robustness into account and imposes a smoothness constraint on the filter transmittances, rather than restricting them to a certain functional form.

We attack this problem simultaneously from the perspective of both the filter design in the measurement device and the mapping in the color calibration. Following Wolski et al,[8] we formulate the task as a constrained optimization problem. The main differences between our work and that in Ref. 8 are the role of illuminants and the implementation. In Ref. 8, the device operates in two modes: emissive or reflective. The samples are either self-luminous or illuminated by the LEDs of the device. The training set is a collection of spectral data. In our work, in order to provide the flexibility of selecting both the input and output illumination conditions in our colorimetry system, it is crucial to factor out illuminants in the derivation. Our training set is restricted to a collection of reflectances.

Wolski et al also did not report any actual measurement results. Their methodology is verified through simulation only. In this paper, we verify our method with experiments. We measure the camera sensitivities and use them to design an appropriate set of filters. To ensure that the designed filters are realizable, we search among a candidate set of Kodak Wratten filters that are currently available on the market to design a 2-exposure 5-illuminant system. We present experimental results in Sec. 3.

2. Multi-exposure colorimetry system

In this section, we describe the design of a multi-exposure colorimetry system using a digital camera. For simplicity, let us start with the multi-exposure single-illuminant system shown in Fig. 1.

2.1. Multi-exposure single-illuminant system

Let N_f be the number of filters in the measurement device; and let $\boldsymbol{F}$ be an augmented matrix

$$\boldsymbol{F} = \left[\ [\boldsymbol{f}_1]\boldsymbol{D} \ \middle|\ [\boldsymbol{f}_2]\boldsymbol{D} \ \middle|\ \cdots \ \middle|\ [\boldsymbol{f}_{N_f}]\boldsymbol{D}\ \right]_{31\times 3N_f}, \quad (1)$$

which characterizes the camera-filter combination of the system. Let $\boldsymbol{r}_k$ be the reflectance of kth color training sample, $k = 1, \ldots, N_r$, and $\boldsymbol{R}$ be the stack of those reflectances,

$$\boldsymbol{R} = [\boldsymbol{r}_1^t\ \boldsymbol{r}_2^t\ \cdots\ \boldsymbol{r}_{N_r}^t]^t. \quad (2)$$

Now, let $\boldsymbol{S}$ be the stack of device outputs which are the filtered camera RGB's of the above N_r training samples taken under illuminant $\boldsymbol{L}$; and let $\boldsymbol{T}'$ be the stack of their true CIE XYZ tristimulus values under illuminant $\boldsymbol{L}'$. That is,

$$\boldsymbol{S} = \begin{bmatrix} R_1^{(1)} & G_1^{(1)} & B_1^{(1)} & \cdots & R_1^{(N_f)} & G_1^{(N_f)} & B_1^{(N_f)} \\ R_2^{(1)} & G_2^{(1)} & B_2^{(1)} & \cdots & R_2^{(N_f)} & G_2^{(N_f)} & B_2^{(N_f)} \\ \vdots & \vdots & \vdots & & \vdots & \vdots & \vdots \\ R_{N_r}^{(1)} & G_{N_r}^{(1)} & B_{N_r}^{(1)} & \cdots & R_{N_r}^{(N_f)} & G_{N_r}^{(N_f)} & B_{N_r}^{(N_f)} \end{bmatrix}.$$

$$\boldsymbol{T}' = \begin{bmatrix} X_1' & Y_1' & Z_1' \\ X_2' & Y_2' & Z_2' \\ \vdots & \vdots & \vdots \\ X_{N_r}' & Y_{N_r}' & Z_{N_r}' \end{bmatrix}. \quad (3)$$

Therefore, the stacks $\boldsymbol{S}$ and $\boldsymbol{T}'$ can be written as

$$\boldsymbol{S} = \boldsymbol{RLF}, \text{and } \boldsymbol{T}' = \boldsymbol{RL}'\boldsymbol{A}, \quad (4)$$

respectively.

Consider the kth color sample for the moment. Its true tristimulus values under $\boldsymbol{L}'$ are

$$\boldsymbol{t}'_k = \boldsymbol{r}_k \boldsymbol{L}' \boldsymbol{A}; \quad (5)$$

and its estimate from the calibration matrix $\boldsymbol{M}'$ is

$$\widehat{\boldsymbol{t}'_k} = \boldsymbol{r}_k \boldsymbol{L} \boldsymbol{F} \boldsymbol{M}'. \quad (6)$$

Hence, the estimation error in CIE XYZ space is

$$\Delta \boldsymbol{t}'_k = \boldsymbol{t}'_k - \widehat{\boldsymbol{t}'_k} = \boldsymbol{r}_k (\boldsymbol{L}' \boldsymbol{A} - \boldsymbol{L} \boldsymbol{F} \boldsymbol{M}'). \quad (7)$$

Applying the same local linearization technique as in Ref. 8, the estimation error $\Delta \boldsymbol{u}'_k$ in CIE $L^*a^*b^*$ space can be approximated by weighting $\Delta \boldsymbol{t}'_k$ with a local Jacobian matrix $\boldsymbol{J}'_k$. That is,

$$\Delta \boldsymbol{u}'^t_k \approx \boldsymbol{J}'_k \Delta \boldsymbol{t}'^t_k = \boldsymbol{J}'_k (\boldsymbol{A}^t \boldsymbol{L}' - \boldsymbol{M}'^t (\boldsymbol{L}\boldsymbol{F})^t) \boldsymbol{r}^t_k. \quad (8)$$

For convenience, we refer to $\Delta E'_k = \|\Delta \boldsymbol{u}'^t_k\|_2$ as the perceptual error, recognizing that the CIE $L^*a^*b^*$ space only accounts for a very limited part of how humans perceive color.

Now let us sum the errors for all the color samples in the training set. The square of the total root-mean-squared error can be approximated by

$$(\Delta E'_{\text{rms}})^2 \approx \|\boldsymbol{B}'_{eq} \text{vec}(\boldsymbol{A}^t \boldsymbol{L}' - \boldsymbol{M}'^t (\boldsymbol{L}\boldsymbol{F})^t)\|_2^2. \quad (9)$$

where,

$$\boldsymbol{B}'^t_{eq} \boldsymbol{B}'_{eq} = \frac{1}{N_r} \sum_{k=1}^{N_r} \boldsymbol{B}'^t_k \boldsymbol{B}_k, \text{ with } \boldsymbol{B}'_k = (\boldsymbol{r}^t_k \otimes \boldsymbol{J}'_k)$$

summarizes the contribution of the training set.

To investigate the robustness of the device, replacing $\boldsymbol{F}$ in Eq. (9) by $\boldsymbol{F} + \Delta \boldsymbol{F}$, then using linearity of vec$(\cdot)$ and two 2-norm inequalities,[8] it can be shown that $(\Delta E'_{\text{rms}})^2$ is upper bounded by $2\varepsilon'_t$,

$$(\Delta E'_{\text{rms}})^2 \le 2\varepsilon'_t. \quad (10)$$

where,

$$\varepsilon'_t = \left\| \begin{bmatrix} \boldsymbol{B}'_{eq} \text{vec}(\boldsymbol{A}^t \boldsymbol{L}') \\ \boldsymbol{0} \end{bmatrix} - \begin{bmatrix} \boldsymbol{B}'_{eq} (\boldsymbol{L}\boldsymbol{F} \otimes \boldsymbol{I}_3) \\ \sqrt{K_t} \boldsymbol{I}_{9n} \end{bmatrix} \text{vec}(\boldsymbol{M}'^t) \right\|_2^2, \quad (11)$$

$$K_t = \|\boldsymbol{B}'_{eq} (\boldsymbol{L} \Delta \boldsymbol{F} \otimes \boldsymbol{I}_3)\|_2^2. \quad (12)$$

For filter smoothness, we define a penalty function ε_s such that

$$\varepsilon_s = K_s \sum_i \|\boldsymbol{D}^2 \boldsymbol{f}_i\|_2^2, \quad (13)$$

using a second order difference operator $\boldsymbol{D}^2$ described in Ref. 8. Consequently, a cost function $h(\boldsymbol{F})$ involving perceptual errors in CIE $L^*a^*b^*$ space, system robustness, and filter smoothness is obtained; and the calibration problem can thus be formulated as the following constrained optimization problem:

Minimize

$$h(\boldsymbol{F}) = \varepsilon'_t + \varepsilon_s, \quad (14)$$

Subject to

$$0 \le \text{all elements of } \boldsymbol{f}_i \le 1 \qquad i = 1, 2, \ldots, N_f.$$

Note that due to the local linearization in Eq. (8), Eq. (11) has a closed-form solution for $\boldsymbol{M}'$ given $\boldsymbol{F}$. It can be computed by

$$\text{vec}(\boldsymbol{M}'^t) = [(\boldsymbol{L}\boldsymbol{F} \otimes \boldsymbol{I}_3)^t \boldsymbol{B}'^t_{eq} \boldsymbol{B}'_{eq} (\boldsymbol{L}\boldsymbol{F} \otimes \boldsymbol{I}_3)]^{-1} \cdot (\boldsymbol{L}\boldsymbol{F} \otimes \boldsymbol{I}_3)^t \boldsymbol{B}'^t_{eq} \boldsymbol{B}'_{eq} \text{vec}(\boldsymbol{A}^t \boldsymbol{L}'). \quad (15)$$

This simplifies the optimization problem and accelerates the search for the solution at the expense of small perceptual errors.

Finally, the constrained optimization problem in Eq. (14) is solved numerically and iteratively using the routine *constr.m* from MATLAB. Note that K_t, K_s, and an initial filter set have to be pre-specified.

2.2. Multi-exposure multi-illuminant system

The extension of the system in Sec. 2.1 to the multi-illuminant case is straightforwardly done by using the following substitutions in the derivation. First replace the output illuminant $\boldsymbol{L}'$, calibration matrix $\boldsymbol{M}'$, and cost term ε'_t by illuminants $\boldsymbol{L}_i$, calibration matrices $\boldsymbol{M}_i$, and cost terms $\varepsilon^{(i)}_t$ for $i = 1, 2, \ldots, m$, respectively. Then the overall cost function $h(\boldsymbol{F})$ is set to

$$h(\boldsymbol{F}) = \max_i \{\varepsilon^{(i)}_t\} + \varepsilon_s, \quad (16)$$

which is equivalent to taking the worst case scenario among illuminants as the overall cost. The optimization can be solved iteratively in a fashion similar to that used in Sec. 2.1.

3. Simulations and experimental results

To implement this colorimetry system, we measured the sensitivity of our DCS460c camera using a tunable monochromatic light source and a spectroradiometer,[9] and utilized a reference data set R1 to design an appropriate filter set for the measurement device. This reference data set consists of DuPont paint chips, Munsell color chips, and natural objects, and is collected from the literature.† As shown in Fig. 2, by performing principal component analysis on this data collection under various illuminants, we

† http://www4.ncsu.edu/eos/users/h/hjt/colordata/obj_spectra/
http://198.53.144.31/~poynton/notes/color/Haanpalo.html

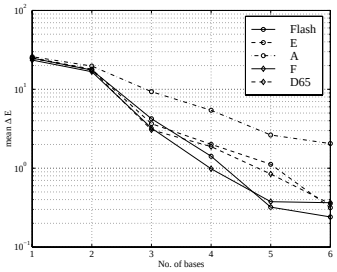

Figure 2: *Principal Component Analysis of the reference data set R1.*

found that 4∼6 basis terms are adequate to achieve a mean ΔE of less than 2 ΔE_{ab} units in approximating the spectral power distributions of those samples. Therefore, we chose to realize a two-exposure colorimetry system which corresponds to a six channel device. This system takes pictures of a color sample illuminated by the camera flash and returns the CIE XYZ tristimulus values of that sample under five pre-specified illuminants: flashlight, equal-energy illuminant E, illuminant A, fluorescent light F, and illuminant D_{65}. The pictures are taken under flashlight because this is the most common light source in photography. The pre-specified illuminants are chosen from a set of commonly encountered light sources to illustrate the performance of the system.

Prior to the system design, a suitable weighting pair (K_t, K_s) has to be specified. In order to do so, we investigated a simplified two-exposure system where the sample is illuminated by a flashlight and the calibration system returns the CIE XYZ tristimulus values under flashlight only. We designed nine filter-calibration matrix pairs for various (K_t, K_s) values, investigated the system performance versus weighting parameter values, and found that $(K_t, K_s) = (10^{-4}, 1)$ is appropriate for this application. The filter transmittances $(\boldsymbol{f}_1, \boldsymbol{f}_2)$ of this optimal filter pair are shown in Fig.3a; and the simulation results are listed in Table 1a. We also tested the robustness of the overall system by adding uniformly distributed random noise $\sim U[-0.005, 0.005]$ to the simulated camera outputs. The strength of this noise corresponds to a $\pm 0.5\%$ device measurement error. The simulation results for the noisy system are also listed in Table 1a.

For the design of the 2-exposure 5-illuminant system, we followed the procedure described in Sec. 2.2, set $(K_t, K_s) = (10^{-4}, 1)$, and found a pair of optimal filters $(\boldsymbol{f}_1^{(o)}, \boldsymbol{f}_2^{(o)})$ whose transmittances are shown in Fig. 3b. The simulation results for this system are listed in Table 1b.

In practice, it is not clear if the designed filters are realizable even with the smoothness penalty ε_s in our problem formulation. To overcome this, we use a suboptimal approach referred to as restricted search. Instead of solving a constrained optimization, we search for the best filter pair among a candidate set of filters that are currently available on the market. One of the two search strategies, exhaustive search and iterated condition modes (ICM),[10] is employed depending on the computational complexity of the problem.

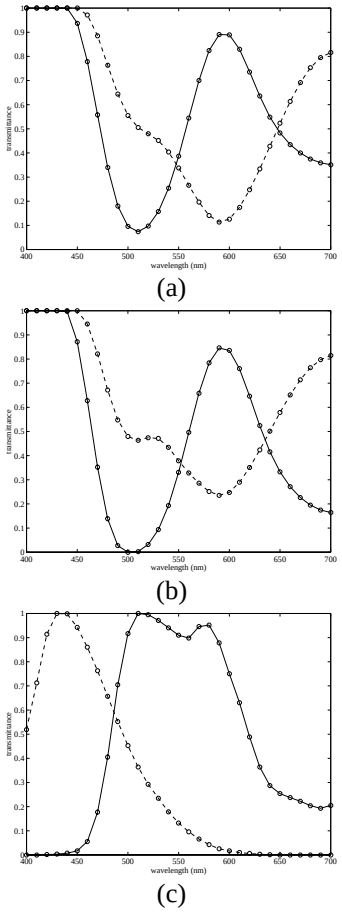

Figure 3: *Optimal filter pairs (a)* $(\boldsymbol{f}_1, \boldsymbol{f}_2)$*, (b)* $(\boldsymbol{f}_1^{(o)}, \boldsymbol{f}_2^{(o)})$*, and (c)* $(\boldsymbol{f}_1^{(w)}, \boldsymbol{f}_2^{(w)})$ *when* $(K_t, K_s) = (10^{-4}, 1)$*. Here, (a) was designed for a 2-exposure Flash-Flash colorimetry system; (b) was designed for a 2-exposure Flash-*$\{$*Flash, E, A, F,* $D_{65}\}$ *colorimetry system using the optimal procedure described in the text; and (c) was designed for a Flash-*$\{$*Flash, E, A, F,* $D_{65}\}$ *colorimetry system using the optimal procedure with the restriction that the filters are combination from the Wratten set. The filters in (c) were realized by (WR11+WR85N6,WR38A+WR80B).*

We applied this methodology to a 2-exposure 5-illuminant system using the reference data set R1 as training samples, and searched among nearly 4000 filter candidates formed by either a single Wratten filter[‡] or a pair of Wratten filters concatenated as one. The two filters that resulted from this restricted search can be realized by four Wratten filters. One is formed by concatenating WR11 and WR85N6; and the other is formed by concatenating WR38A and WR80B.

[‡] http://www4.ncsu.edu/eos/users/h/hjt/colordata/

The filter transmittances $(\boldsymbol{f}_1^{(w)}, \boldsymbol{f}_2^{(w)})$ of this suboptimal solution are shown in Fig. 3c; and the simulation results for this system are shown in Table 1c. From Table 1b and 1c, it is observed that with a large set of filter candidates, the performance of the system is degraded only slightly when applying restricted search rather than optimal design. With respect to implementation, this is an encouraging observation.

	Flash	E	A	F	D_{65}	max.
$\overline{\Delta E_1}$	0.21	0.51	0.27	0.45	0.41	0.51
$\overline{\Delta E_2}$	2.64	3.44	2.06	3.07	3.30	3.44
$\overline{\Delta E_3}$	2.78	3.61	2.16	3.17	3.50	3.61

(a)

	Flash	E	A	F	D_{65}	max.
$\overline{\Delta E_1}$	0.11	0.38	0.24	0.35	0.28	0.38
$\overline{\Delta E_2}$	2.56	2.98	2.29	2.61	2.92	2.98
$\overline{\Delta E_3}$	2.67	3.09	2.39	2.72	3.05	3.09

(b)

	Flash	E	A	F	D_{65}	max.
$\overline{\Delta E_1}$	0.41	0.70	0.39	0.73	0.61	0.70
$\overline{\Delta E_2}$	2.57	3.18	3.11	3.37	2.70	3.37
$\overline{\Delta E_3}$	2.67	3.31	3.27	3.49	2.79	3.49

(c)

Table 1: Simulated performance of a 2-exposure colorimetry system using filters (a) $(\boldsymbol{f}_1, \boldsymbol{f}_2)$, (b) $(\boldsymbol{f}_1^{(o)}, \boldsymbol{f}_2^{(o)})$, and (c) $(\boldsymbol{f}_1^{(w)}, \boldsymbol{f}_2^{(w)})$ from Fig. 3. The calibration matrices $\boldsymbol{M}_i$ $i = 1, \ldots, 5$, were computed from Eq. (15). In this table, all 1559 object reflectances in R1 were employed to calculate the calibration matrices. $\overline{\Delta E_1}$ is the mean perceptual error between the true tristimulus values and the estimate from the corresponding $\boldsymbol{M}_i$ for a given illuminant $\boldsymbol{L}_i$. $\overline{\Delta E_2}$ is the average mean perceptual error over 100 trials. The mean perceptual error in each trial is the error between the true tristimulus value and the estimate from $\boldsymbol{M}_i$ in the presence of random noise $\sim U[-0.005, 0.005]$. $\overline{\Delta E_3}$ is the maximum mean perceptual error from these 100 trials. Hence, $\overline{\Delta E_1}$ indicates the performance of the system without measurement noise, $\overline{\Delta E_2}$ indicates the robustness of the system, and $\overline{\Delta E_3}$ indicates the worst case scenario.

We implemented the multi-exposure camera system using Wratten filters $(\boldsymbol{f}_1^{(w)}, \boldsymbol{f}_2^{(w)})$ and evaluated its performance by conducting experiments on 278 Munsell color chips illuminated by daylight in a Macbeth SpectraLight II viewing booth. We shall refer to this set as the testing set T1. In our experiment, the pictures were taken under daylight rather than camera flash because we did not have the capability to synchronize the shutter of our spectroradiometer and the camera flash. The experimental results are listed in Table 2. Note that the calibration matrices were computed prior to the experiment using the data set R1. None of the test samples in T1 were involved in this computation.

Even though the calibration matrices can be pre-computed, a scaling procedure is necessary since the calibration matrices calculated from Eq. (15) are not invariant to the camera exposure time and the distance from the sample to the camera. We used the following procedure. First, we took pictures of a sample with known reflectance $\boldsymbol{r}_w$ using the digital camera with the ith filter $\boldsymbol{f}_i$ to acquire the data $R_w^{(i)}, G_w^{(i)}$, and $B_w^{(i)}$, $i = 1, 2, \ldots, N_f$. Then we computed the scaling factors $\rho_R^{(i)}, \rho_G^{(i)}$, and $\rho_B^{(i)}$ for the ith exposure by taking the ratio between the simulated camera outputs $\boldsymbol{r}_w \boldsymbol{L} \text{diag}(\boldsymbol{f}_i) \boldsymbol{D}_j$, $j = R, G, B$ and the measured camera outputs $R_w^{(i)}, G_w^{(i)}$, and $B_w^{(i)}$ of that sample. That is,

$$\begin{bmatrix} \rho_R^{(i)} \\ \rho_G^{(i)} \\ \rho_B^{(i)} \end{bmatrix} = \begin{bmatrix} (\boldsymbol{r}_w \cdot \boldsymbol{L} \cdot \text{diag}(\boldsymbol{f}_i) \cdot \boldsymbol{D}_R)/R_w^{(i)} \\ (\boldsymbol{r}_w \cdot \boldsymbol{L} \cdot \text{diag}(\boldsymbol{f}_i) \cdot \boldsymbol{D}_G)/G_w^{(i)} \\ (\boldsymbol{r}_w \cdot \boldsymbol{L} \cdot \text{diag}(\boldsymbol{f}_i) \cdot \boldsymbol{D}_B)/B_w^{(i)} \end{bmatrix}. \quad (17)$$

Here, $\boldsymbol{D}_R, \boldsymbol{D}_G$, and $\boldsymbol{D}_B$ are 31×1 camera sensitivities in the red, green, and blue channels. Note that $\boldsymbol{r}_w$ is 1×31. The pre-computed calibration matrices are then adjusted by pre-multiplication with the scaling matrix

$$\boldsymbol{M}_S = \text{diag}\left(\rho_R^{(1)}, \rho_G^{(1)}, \rho_B^{(1)}, \ldots, \rho_R^{(N_f)}, \rho_G^{(N_f)}, \rho_B^{(N_f)}\right). \quad (18)$$

For completeness, we applied the regression method (see Ref. 5) with our multi-exposure camera system as well. Half of the samples in T1 were randomly selected as the training set for computing calibration matrices

$$\boldsymbol{M}_i = (\boldsymbol{S}^t \boldsymbol{S})^{-1} \boldsymbol{S} \boldsymbol{T}_i, \qquad i = 1, 2, \ldots, 5. \quad (19)$$

They are then applied to the entire set T1. The experimental results are shown in Table 3.

4. Discussion

The filters for system 1a were designed for flash-flash only; whereas the filters for system 1b were designed to minimize the maximum error under 5 illuminants. Therefore we expect, as observed from Tables 1a and 1b, that the worst case errors for 1b will be less than those for 1a. On the other hand, we would also expect that under flash illumination, the errors for system 1a should be less than those for system 1b. However, by comparing Eqs. (14) and (16), we see that the cost term ε_s is relatively more important in the single-illuminant case than in the multi-illuminant case since we took the maximum value of the cost terms $\varepsilon_t^{(i)}$ in the latter case. As a result, system 1a has a smoother filter pair, but does not perform better than system 1b under the flashlight.

By comparing Tables 1b and 2, it is obvious that the experimental results are degraded with respect to the simulation results. This is because 1) there exist various sources of error including the measurement of camera sensitivities and filter transmittances, the camera outputs themselves, and the tristimulus measurement using the spectroradiometer, and 2) the filter sets are designed for pictures taken under the camera flash rather than under the daylight.

	Flash	E	A	F	Daylight	max.
$\overline{\Delta E}$	4.46	4.98	4.70	5.86	4.60	5.86

Table 2: Experimental results for a 2-exposure 5-illuminant colorimetry system using Wratten filters, WR11+WR85N6 and WR38A +WR80B. The test samples in T1 were illuminated under daylight in a Macbeth viewing booth. In this colorimetry system, the calibration matrices $\boldsymbol{M}_i$ $i = 1, \ldots, 5$, were computed off line from Eq. (15) using data of (i) the measured spectral power distribution of the daylight, (ii) the measured transmittance of $(\boldsymbol{f}_1^{(w)}, \boldsymbol{f}_2^{(w)})$ in Fig. 3c, (iii) the collected reflectances in R1, and (iv) the measured scaling factors for each channel. Note that the pictures of the test samples were taken under daylight. These RGB's were then employed to estimate the tristimulus values using $\boldsymbol{M}_i$.

	Flash	E	A	F	Daylight	max.
$\overline{\Delta E}$	1.78	1.85	1.85	1.97	1.83	1.97

Table 3: Experimental results for a 2-exposure 5-illuminant colorimetry system using Wratten filters, WR11+WR85N6 and WR38A +WR80B. The test samples in T1 were illuminated under daylight in a Macbeth viewing booth. In this colorimetry system, the calibration matrices $\boldsymbol{M}_i$ $i = 1, \ldots, 5$, were computed by the regression method described in Ref. 5, using half of the samples in T1 and Eq. (19). These matrices were then applied to the entire T1 set.

Comparing Tables 2 and 3, we see that the regression-based method performs better than our model-based method. This is because the model-based approach is affected by errors in measuring camera sensitivities and filter transmittances, while the regression-based method is not. However, the model-based approach provides a basis for designing the filters in the measurement device, whereas the regression-based approach can only operate when the measurement device is given. Furthermore, the model-based approach is more flexible. Unlike the regression-based method, its calibration matrices can be easily updated without any calibration effort. For example, if we want to apply the same multi-exposure camera system to assess the color of human teeth, the calibration matrices can be updated by choosing a reference data set R1 that contains only the reflectances of human teeth and re-computing Eq. (15). When we apply the regression method for the same scenario, it is necessary to acquire a training set of camera data from human teeth before the calibration matrices can be updated.

5. Conclusion

In this paper, we proposed a methodology for utilizing digital cameras for imaging colorimetry. This technique requires little effort in color calibration once the system characteristics are identified. Our method possesses several advantages. First of all, it takes several important issues such as system robustness, filter smoothness, and perceptual errors in color assessment into account. Secondly, the calibration matrices can be pre-computed with a suitable collection of reflectances R1. Finally, this method allows great flexibility in application-dependent design when the illumination conditions and the reference data collection R1 are properly chosen. We verified our technique by implementing a colorimetry system for general purpose color assessment and conducting experiments on 278 Munsell color chips.

References

1. G. Wyszecki and W. Stiles, *Color Science: concepts and methods, quantitative data and formulae*, John Wiley & Sons, Inc, **2**, 1982.
2. J. Farrell, D. Sherman, and B. Wandell, How to turn your scanner into a colorimeter, *IS&T's Tenth Int. Congress on Advances in Non-impact Printing Technologies*, pp. 579-581, 1994.
3. Shoji Tominaga, Spectral Imaging by a Multi-Channel Camera, *SPIE*, **3648**, pp. 38-47, 1999.
4. H. Haneishi, T. Hasegawa, N. Tsumura, and Y. Miyake, Design of Color Filters for Recording Artworks, *IS&T's 50th Annual Conference*, pp. 369-372, 1995.
5. W. Wu, J. P. Allebach, and M. Analoui, Using a Digital Camera for Colorimetry of Human Teeth, *Proc. PICS*, pp. 37-42, 1998.
6. G.D. Finlayson and M.S. Drew, The Maximum Ignorance Assumption with Positivity, *The Fourth Color Imaging Conference: Color Science, Systems and Applications*, pp. 202-205, 1996.
7. P. Chen and H. J. Trussell, Color Filter Design for Multiple Illuminants and Detectors, *Proc. of the IS&T/SID 1995 Color Imaging Conference: Color Science, Systems and Applications*, pp. 67-70, 1995.
8. M. Wolski, C. A. Bouman, J. P. Allebach, and E. Walowit, Optimization of Sensor Response Functions for Colorimetry of Reflective and Emissive Objects, *IEEE Transactions on Image Processing*, **5**(**3**), pp. 507-517, 1996.
9. P. M. Hubel, D. Sherman, and J. E. Farrell, A Comparison of Methods of Sensor Spectral Sensitivity Estimation *IS&T/SID's 2nd Color Imaging Conference: Color Science, Systems and Applications*, pp. 45-48, 1994.
10. J. Besag, On the statistical analysis of dirty pictures, *J. Roy. Statist. Soc. B*, **48**(**3**), pp. 259-302, 1986.